Computational Structural Engineering
An International Journal
Vol. 2, No. 1, pp. 33~42 (2002)

Computational Structural Engineering Institute

Computational Soil-Structure Interaction Design via Inverse Problem Formulation for Cone Models

Izuru Takewaki†, Hiroshi Fujimoto and Koji Uetani

Department of Architecture and Architectural Systems, Graduate School of Engineering, Kyoto University, Sakyo, Kyoto 606-8501, Japan

Received May 2002; Accepted July 2002

ABSTRACT

A computationally efficient stiffness design method for building structures is proposed in which dynamic soil-structure interaction based on the wave-propagation theory is taken into account. A sway-rocking shear building model with appropriate ground impedances derived from the cone models due to Meek and Wolf (1994) is used as a simplified design model. Two representative models, i.e. a structure on a homogeneous half-space ground and a structure on a soil layer on rigid rock, are considered. Super-structure stiffnesses satisfying a desired stiffness performance condition are determined via an inverse problem formulation for a prescribed ground-surface response spectrum. It is shown through a simple yet reasonably accurate model that the ground conditions, e.g. homogeneous half-space or soil layer on rigid rock (frequency-dependence of impedance functions), ground properties (shear wave velocity), depth of surface ground, have extensive influence on the super-structure design.

Keywords: stiffness design, inverse vibration problem, structure-foundation-soil interaction, cone model, soil layer on rigid rock, wave propagation, design response spectrum

1. Introduction

The problem of soil-structure interaction (SSI) is very important in identifying the damage to building structures under strong ground motions and clarifying the input mechanism of actual effective ground motions into the building structures. Most of the SSI problems have been solved theoretically or numerically and many useful observations and implications have been accumulated (see for example, Luco, 1980; Cakmak *et al.*, 1982; Wolf, 1985; Cakmak, 1987; Wolf, 1988; Cakmak and Herrera, 1989; Gupta and Trifunac, 1991; Meek and Wolf, 1994; Wolf, 1994; Kausel and Manolis, 2000). However, it may be true that most of the previous analysis techniques are too complicated and/or time-consuming. It is also true that, while analysis methods of the SSI effects have been well established, the corresponding design methods for building structures have never been developed except a few attempts by the present authors (Nakamura and Takewaki, 1985, 1989b; Nakamura *et al.*, 1992, 1996; Takewaki, 1998; Takewaki and Nakamura, 1995, 1997; Takewaki *et al.*, 1998, 2002). It is therefore not necessarily easy for structural designers to incorporate the essential features of the SSI effects into their usual structural design practice. To tackle this problem in a smart manner, some attempts have been conducted by introducing simplified models or techniques. Simplicity of the computational procedure together with its accuracy is an important issue in the practical structural design. Among them, the cone model due to Meek and Wolf (1994) may be a simple yet reasonably accurate model. In this paper, this cone model is used to take into account the SSI effects in the design process.

The purpose of this paper is to propose a new computationally efficient stiffness design method for building structures taking into account the various aspects of the SSI effects. A sway-rocking shear building model with appropriate ground impedances derived from the cone model is introduced as a simplified design model and super-structure stiffnesses satisfying a desired stiffness performance condition are determined for a prescribed

† Corresponding author
Tel.: +81-75-753-4762; Fax: +81-75-753-5748
E-mail address: takewaki@archi.kyoto-u. ac.jp

ground-surface response spectrum. An inverse vibration formulation is developed in the process of the super-structure stiffness design in which the fundamental natural frequency of the interaction model is regarded as a principal design parameter. It is shown that the ground conditions, e.g. homogeneous half-space or soil layer on rigid rock (frequency-dependence of impedance functions), ground properties (shear wave velocity), depth of surface ground, have extensive influence on the super-structure design. It should be noted that the previous papers (Nakamura and Takewaki, 1985, 1989b; Nakamura *et al.*, 1992, 1996; Takewaki, 1998; Takewaki and Nakamura, 1995, 1997; Takewaki *et al.*, 1998, 2002) do not present methods for incorporating the properties of three-dimensional wave-propagation within a reasonable amount of computational resources and a reasonable accuracy.

2. Design Problem

Consider a shear building model supported by a flat-slab foundation on a homogeneous visco-elastic half-space or on a homogeneous soil layer on a rigid rock. The viscosity of the ground will be considered approximately by adding the viscous damping ratio to the radiation damping ratio evaluated via the cone models. The former model is called the half-space model (see Fig. 1(a)) and the latter is called the soil layer model (see Fig. 1(b)). It is noted that, while a homogeneous half-space ground has often been utilized in computing foundation impedances in usual structural design practice, the evaluation of impedance functions for the soil layer model taking into account the three-dimensional wave propagation is not so simple and easy. Such difficulty is overcome by introducing the cone models due to Meek and Wolf (1994). Both design models are modeled as a shear building model supported by a swaying and rocking spring-dashpot system. The objective of the design problem is to find the story stiffnesses of a model which exhibits a specified mean peak interstory drift $\bar{\delta}$ (or story drift angle=$\bar{\delta}$/(story height)) to the design earthquake.

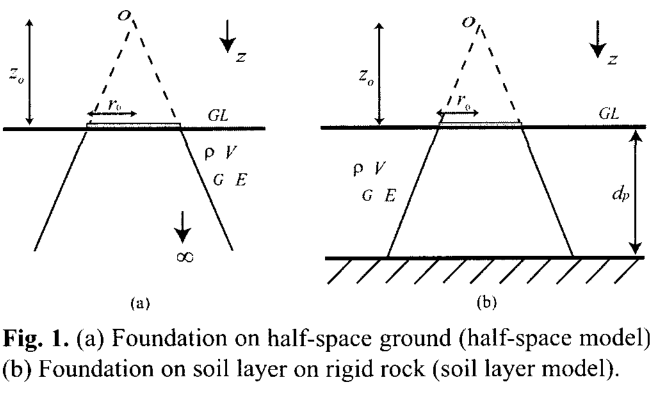

Fig. 1. (a) Foundation on half-space ground (half-space model) (b) Foundation on soil layer on rigid rock (soil layer model).

The design earthquake is defined at the ground surface level in terms of a design displacement response spectrum. The design displacement response spectrum $S_D(T;h)$ (Newmark and Hall, 1982) is defined by

$$S_D^{(1)}(T;h) = \ddot{u}_{g\,\max}(3.21-0.68\,ln(100h))\left(\frac{T}{2\pi}\right)^2 (T \le T_L)$$

$$S_D^{(2)}(T;h) = \dot{u}_{g\,\max}(2.31-0.41\,ln(100h))\left(\frac{T}{2\pi}\right)(T_L \le T \le T_U)$$

$$S_D^{(3)}(T;h) = u_{g\,\max}(1.82-0.27\,ln(100h))(T_U \le T) \qquad (1)$$

where T and h denote the natural period and damping ratio. T_L and T_U are determined from $S_D^{(1)}(T_L;h) = S_D^{(2)}(T_L;h)$ and $S_D^{(2)}(T_U;h) = S_D^{(3)}(T_U;h)$. The maximum ground acceleration $\ddot{u}_{g\,\max}$, velocity $\dot{u}_{g\,\max}$ and displacement $u_{g\,\max}$ are assumed to be 0.804 (m/s^2), 0.100 (m/s) and 0.075 (m), respectively.

3. Foundation Impedance Via Cone Models

A sway-rocking model is used in the stiffness design explained in the next section. It is necessary to evaluate the foundation impedances which will be used as the spring stiffnesses and dashpot damping coefficients of the sway-rocking model. To compute the foundation impedances, the cone model is used (Fig. 1).

The cone model has been proposed by Meek and Wolf (1994) and Wolf (1994) for evaluating the dynamic stiffness and the effective input motion of a foundation on the ground. Compared to more rigorous numerical methods, this cone model requires only simple numerical manipulation within reasonable accuracy. The cone model is based on an assumption that the force transmitting mechanism of a foundation on the ground subjected to dynamic disturbances can be represented approximately by a cone chopped by the foundation. The accuracy investigation of the cone models has been made extensively by Wolf (1994) for various parameter ranges through the comparison with the results due to more rigorous methods. The procedure of evaluating the impedance functions via the cone models is simply described in Appendix 1 and the horizontal and rocking components for Poisson's ratio 0.45 are illustrated in Fig. 2. The soil density, the shear wave velocity, the radius of the circular foundation and the depth of soil layer (soil layer model) are $\rho = 1.6 \times 10^3$ (kg/m^3), $V_S = 200(m/s)$, $r_0 = 10(m)$ and $d_P = 20(m)$.

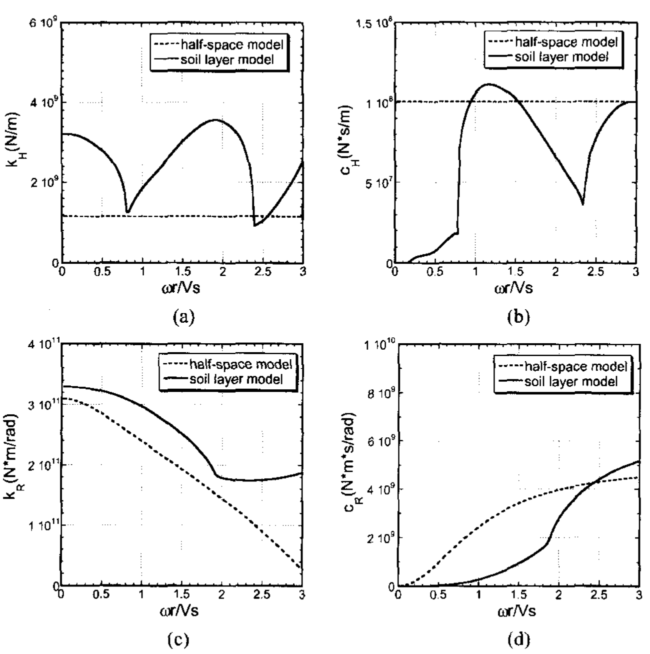

Fig. 2. Impedance functions for half-space model and soil layer model: (a) horizontal stiffness, (b) horizontal damping coefficient (c) rocking stiffness, (d) rocking damping coefficient.

4. Stiffness Design Method Via Inverse Problem Formulation

4.1 Equations of motion for sway-rocking model

Consider an f-story shear building model, as shown in Fig. 3, supported by a swaying and rocking spring-dashpot system. Let u_F and θ_F denote the horizontal displacement and angle of rotation of the ground floor and let $u_1, \ldots, u_f$

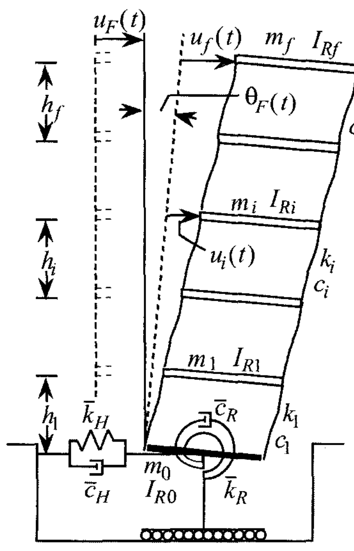

Fig. 3. Shear building model supported by swaying and rocking spring-dashpot system.

denote the horizontal displacements of the upper floors without any rigid-body mode component due to the ground floor (foundation) motion. The set $\{u\}=\{u_1 \ldots u_f\, u_F\, \theta_F\}^T$ is treated as the generalized displacements where $(\ )^T$ denotes the transpose of a vector. Let $\bar{k}_H$ and $\bar{k}_R$ denote the stiffnesses of the swaying and rocking springs and let $\bar{c}_H$ and $\bar{c}_R$ denote the damping coefficients of the swaying and rocking dashpots. The damping coefficients include the radiation damping deriv-ed from the cone models and the material damping of soil. The inter-story drift $\delta_j = u_j - u_{j-1}$ does not include any rigid-body mode component. Let k_j denote the stiffness in the jth story.

Let m_j, I_{Rj}, and H_j denote the mass, the moment of inertia around its centroid and the height of the mass in the jth floor from the ground surface. The story height of the jth story is denoted by h_j. The system mass matrix may be expressed as

$$[M] = \begin{bmatrix} [M_B] & [M_{BH}] & [M_{BR}] \\ & E_1 & E_2 \\ sym. & & E_3 \end{bmatrix} \tag{2}$$

where

$$[M_B] = diag(m_1 \ldots m_f),\ [M_{BH}] = \{m_1 \ldots m_f\}^T,$$
$$[M_{BR}] = \{m_1 H_1 \ldots m_f H_f\}^T \tag{3a-c}$$
$$E_1 = \sum_{i=0}^{f} m_i,\ E_2 = \sum_{i=1}^{f} m_i H_i,\ E_3 = \sum_{i=1}^{f} m_i H_i^2 + \sum_{i=0}^{f} I_{Ri},$$
$$H_i = \sum_{j=1}^{i} h_j \tag{4a-d}$$

The system stiffness matrix may be described as

$$[K] = [K_B] + [K_H] + [K_R] \tag{5}$$

where

$$[K_B] = \begin{bmatrix} k_1+k_2 & -k_2 & & & & & & \\ & \ddots & \ddots & & & & & \\ & & \ddots & -k_i & & & & \\ & & & k_i+k_{i+1} & \ddots & & & \\ & & & & \ddots & -k_{f-1} & & \\ & & & & & k_{f-1}+k_f & -k_f & \\ & & & & & & k_f & 0 \\ sym. & & & & & & 0 & 0 \\ & & & & & & & 0 \end{bmatrix},$$

$$[K_H] = diag(0 \ldots 0\ \bar{k}_H\ 0),\quad [K_R] = diag(0 \ldots 0\ 0\ \bar{k}_R) \tag{6a-c}$$

Let us assume that the damping matrix $[C]$ of the model is expressed as the superposition of the damping matrices of the three parts, i.e., the building, the swaying dashpot and the rocking dashpot. Let c_j denote the damping coefficient in the jth story. It is also assumed here that each subassemblage has a stiffness-proportional damping matrix. Let h_B denote the damping ratio of the shear building model. Let ω_1 denote the undamped fundamental natural circular frequency of the interaction model. The system damping matrix $[C]$ may then be described as

$$[C] = [C_B] + [C_H] + [C_R] \tag{7}$$

where $[C_B](= (2h_B/\omega_1)[K_B])$ is derived by replacing $\{k_j\}$ in $[K_B]$ by $\{c_j\}$ and

$$[C_H] = diag(0\ldots0\ \bar{c}_H\ 0),\ [C_R] = diag(0\ldots0\ 0\ \bar{c}_R) \quad (8a,\ b)$$

This system is subjected to the horizontal ground surface acceleration $\ddot{u}_g$. The equations of motion of the system may be described as

$$[M]\{\ddot{u}\} + [C]\{\dot{u}\} + [K]\{u\} = -M\{q\}\ddot{u}_g \tag{9}$$

The influence coefficient vector $\{q\}$ can be given by

$$\{q\} = \{0\ldots0\ 1\ 0\}^T \tag{10}$$

It should be reminded that the first f equations in equation (9) represent the equations of horizontal equilibrium of the floors except the ground floor and the (f+1)-th equation and (f+2)-th equation represent the equation of horizontal equilibrium as a whole of the building-spring system and that of rotational equilibrium as a whole of the building-spring system around the ground floor, respectively.

4.2 Stiffness design via inverse problem formulation

A formula of story stiffnesses has been derived (Nakamura and Takewaki, 1985; Takewaki, 1998) for a specified fundamental natural circular frequency of a sway-rocking model and a uniform distribution of lowest-mode interstory drifts (see Appendix 2). That formula has been derived originally for fixed spring stiffnesses (frequency-independent values). However, it may also be used in the case where the spring stiffnesses are variable in the frequency range and determined approximately as $\bar{k}_H = k_H(\omega_1)$, $\bar{k}_R = k_R(\omega_1)$, for the fundamental natural circular frequency ω_1. This expression is used in this paper. It is noted that the investigation on the design-space correspondence between the frequency-independent model and the frequency-dependent model is very important (see Nakamura and Takewaki, 1989a).

If it is assumed that the mean peak interstory drifts $\{\delta_{i\max}\}$ of a rather low-rise building can be approximated by a fundamental vibration component in the SRSS estimate (square root of the sum of the squares, Der Kiureghian, 1980), the following relation holds.

$$\delta_{i\max} \cong S_D(T_1; h^{(1)})\gamma_1\mu \tag{11}$$

where μ is the interstory-drift component (uniform in this case) in the lowest eigenmode and γ_1 is the lowest-mode participation factor. T_1 and $h^{(1)}$ are the undamped fundamental natural period and the lowest-mode damping ratio of the sway-rocking model. It is also assumed that the equations of motion of the sway-rocking model can be decomposed approximately into classical normal modes. This assumption has been verified in a fairly wide parameter range by the present authors (Nakamura and Takewaki, 1989b). When the normalization condition of the lowest eigenmode Φ with respect to the mass matrix $[M]$ is employed, μ and γ_1 may be expressed as

$$\mu = \left[m_0U_F^2 + \sum_{i=1}^{f} m_i(U_F + \Theta_F H_i + i)^2 + \sum_{i=1}^{f} I_{Ri}\Theta_F^2\right]^{-\frac{1}{2}} \tag{12}$$

$$\gamma_1 = \left[m_0U_F + \sum_{i=1}^{f} m_i(U_F + \Theta_F H_i + i)\right]\mu \tag{13}$$

U_F and Θ_F are defined in Appendix 2. The lowest-mode damping ratio may then be expressed as

$$h^{(1)} = \frac{1}{2\omega_1}\frac{\Phi^T[C]\Phi}{\Phi^T[M]\Phi}$$
$$= \frac{\mu^2}{2\omega_1}\Big\{c_H(\omega_1)U_F(\omega_1)^2 + c_R(\omega_1)\Theta_F(\omega_1)^2$$
$$+ \sum_{i=1}^{f}\frac{2h_B}{\omega_1}k_i(\omega_1)\Big\} \tag{14}$$

where $c_H(\omega_1), c_R(\omega_1), k_i(\omega_1), U_F(\omega_1), \Theta_F(\omega_1)$ are functions of ω_1.

From equations (11)-(14), $\delta_{i\max}$ can be regarded as a function of the undamped fundamental natural period T_1 of the interaction model. In the present design algorithm, T_1 is regarded as the principal design parameter and it is aimed at finding T_1 such that $\delta_{i\max}$ would coincide with the specified value $\bar{\delta}_i$. It should be pointed out that the present method does not require eigenvalue analysis and facilitates its use in usual structural design practice.

5. Design Examples

It is well-known that soil-structure interaction is remarkable in low-rise building structures. A three-story and five-story shear building models are considered here. The span of the building model is $10(m)$ and each story height is $3.5(m)$. A circular foundation mat of area=$300(m^2)$ is assumed ($r_0 = 9.8(m)$). The masses and moments of inertia are $m_0 = 2.4 \times 10^5(kg), m_i = 0.8 \times 10^5(kg)(i \neq 0)$, I_{R0}=2.0 $\times 10^6(kg \cdot m^2), I_{Ri} = 0.667 \times 10^6(kg \cdot m^2)(i \neq 0)$. The damping ratio 0.02 is considered for the building model.

Four shear wave velocities V_s=50, 100, 200, 400(m/s) are considered. It should be noted that these shear wave velocities should be regarded as equivalent ones taking into account the stiffness reduction of soil with respect to strain level. The density of soil is assumed to be $1.6 \times 10^3(kg/m^3)$. Three depths of surface layer d_P=10, 20, 40(m) are considered. The material damping of soil is expressed in terms of a swaying damping ratio 0.05 (stiffness-proportional viscous damping). This swaying material damping is added to the radiation damping evaluated by the cone model. The specified story drift angle is 1/400.

Figs. 4(a)-(d) are illustrated for the 3-story models for various ground shear wave velocities. Fig. 4(a) shows the mean peak interstory drift given by Eq.(11) with respect to the fundamental natural period of the interaction model for the half-space model. The period for zero interstory drift indicates the fundamental natural period of the rigid model supported by the corresponding soil springs. The fundamental natural period of the interaction model satisfying the stiffness design condition (story drift angle=1/400) can be found directly from Fig. 4(a). This graph is very useful for performance-based design which requires the straightforward determination of story stiffnesses for various response targets. Fig. 4(b) illustrates the corresponding story stiffnesses for the specified story drift angle. Figs. 4(c), (d) shows the corresponding distributions for the soil layer model (d_P=20m). Irregular response properties in Fig. 4(c) for the soil layer model may result from the irregular impedance functions shown in Fig. 2. It can be observed that, as the ground shear wave velocity becomes smaller, the super-structure story stiffness for the specified interstory drift level becomes smaller.

Figs. 5(a)-(d) are shown for the 5-story models corresponding to Figs. 4(a)-(d). The depth of soil layer in the soil layer model is d_P=20 m. A similar tendency to the 3-story model can be observed.

Fig. 6 illustrates the comparison of the half-space model and the soil layer model (d_P=20 m) for the 3-story models. Figs. 6(a), (b) are for the shear wave velocity of 100(m/s) and Figs. 6(c), (d) are for 400(m/s). It can be observed that

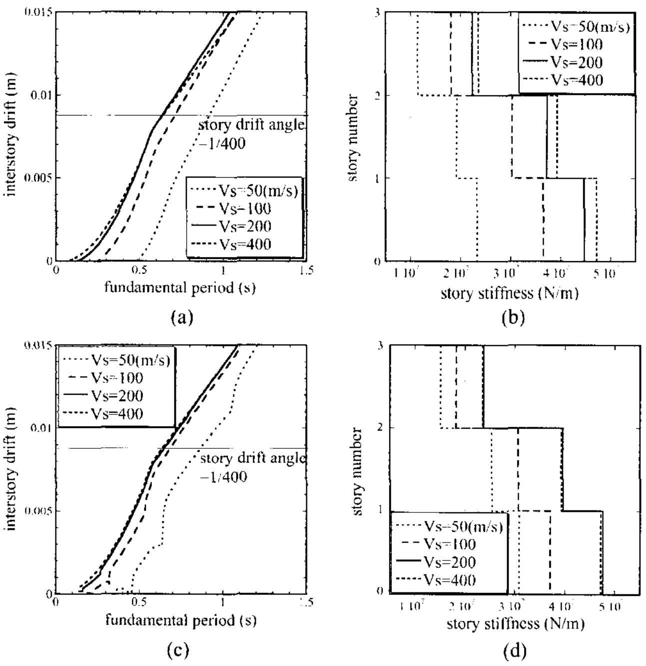

Fig. 4. 3-story model for various shear wave velocities for half-space model and soil layer model: (a) interstory drift vs. fundamental period of interaction model (half-space model), (b) story stiffness (half-space model), (c) interstory drift vs. fundamental period of interaction model (soil layer model), (d) story stiffness (soil layer model).

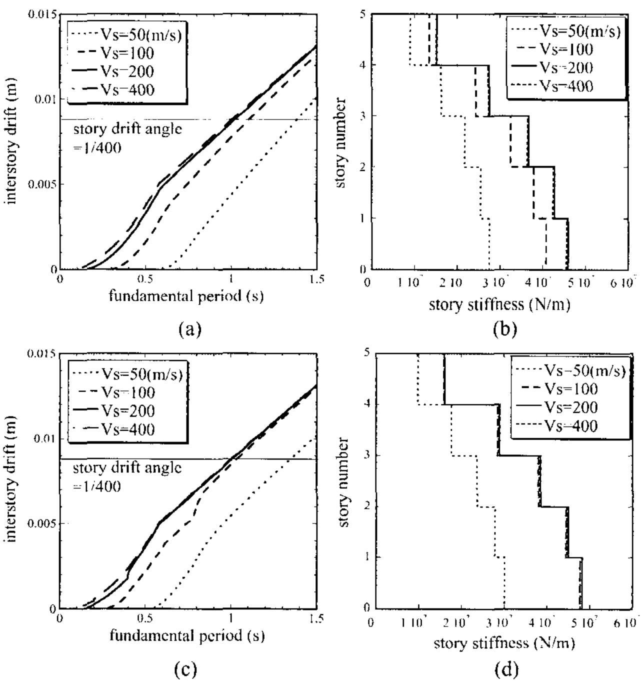

Fig. 5. 5-story model for various shear wave velocities for half-space model and soil layer model: (a) interstory drift vs. fundamental period of interaction model (half-space model), (b) story stiffness (half-space model), (c) interstory drift vs. fundamental period of interaction model (soil layer model), (d) story stiffness (soil layer model).

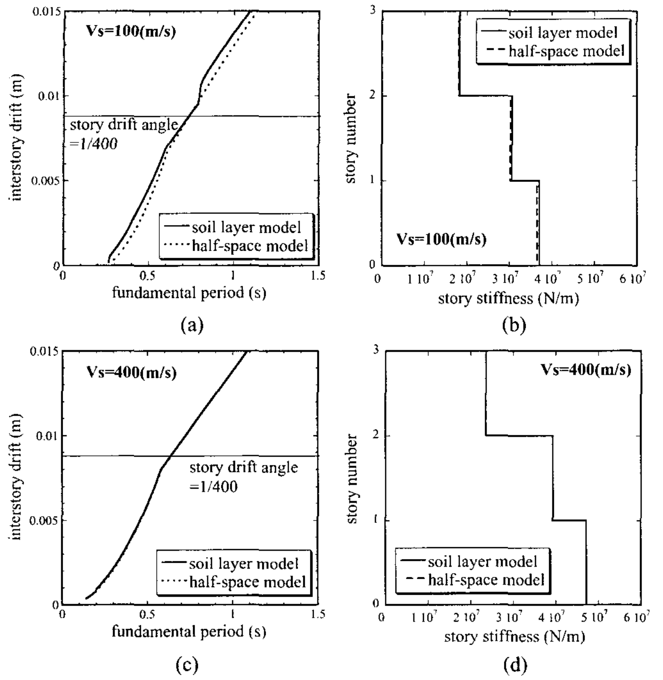

Fig. 6. 3-story model for half-space model and soil layer model: (a) interstory drift vs. fundamental period of interaction model (V_s=100(m/s)), (b) story stiffness (V_s=100(m/s)), (c) interstory drift vs. fundamental period of interaction model (V_s=400(m/s)), (d) story stiffness (V_s=400(m/s)).

a difference exists as the shear wave velocity becomes small.

Fig. 7 shows the corresponding distributions for the 5-story model. The depth of soil layer in the soil layer model is d_p=20 m. It can be observed that larger story stiffnesses are required for the soil layer model. This may result from the complicated combination of horizontal soil spring stiffness and dashpot damping coefficient. The dimensionless frequency corresponding to the fundamental natural period is about 0.6 in this case. While the horizontal soil spring stiffness of the soil layer model is larger than that of the half-space model, the dashpot damping coefficient of the soil layer model due to the radiation damping is much smaller than that of the half-space model (Fig. 2(a), (b)). This small radiation damping of the soil layer model results from the existence of the cut-off frequency.

Fig. 8 shows the comparison for various depths of soil layer for the 3-story model. It can be observed that no clear tendency exists for the difference of depth of soil layer. In this case the depth of 20(m) requires the smallest set of story stiffnesses. This may result from the resonance between the soil layer vibration and the super-structure vibration.

Fig. 9 illustrates the corresponding distributions for the 5-story model. It is interesting to note that, if the specified

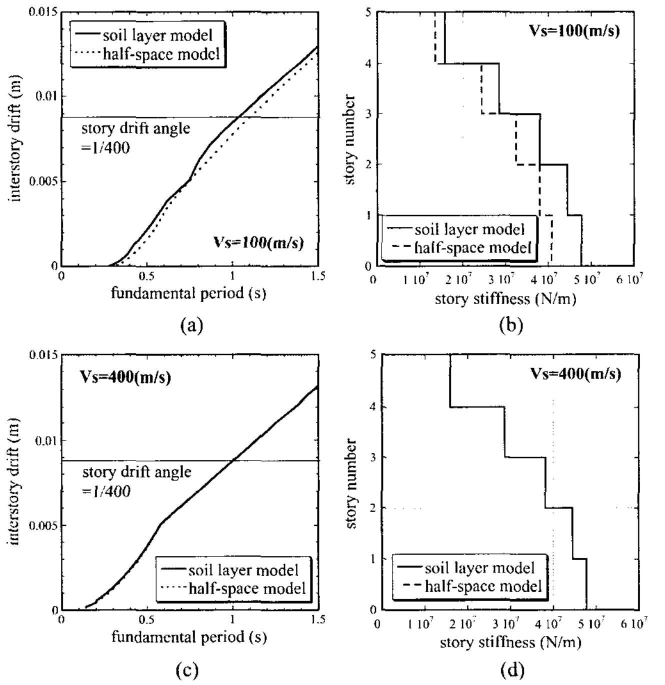

Fig. 7. 5-story model for half-space model and soil layer model (a) interstory drift vs. fundamental period of interaction mode (V_s=100(m/s)), (b) story stiffness (V_s=100(m/s)), (c) interstory drift vs. fundamental period of interaction model (V_s=400(m/s)), (d) story stiffness (V_s=400(m/s)).

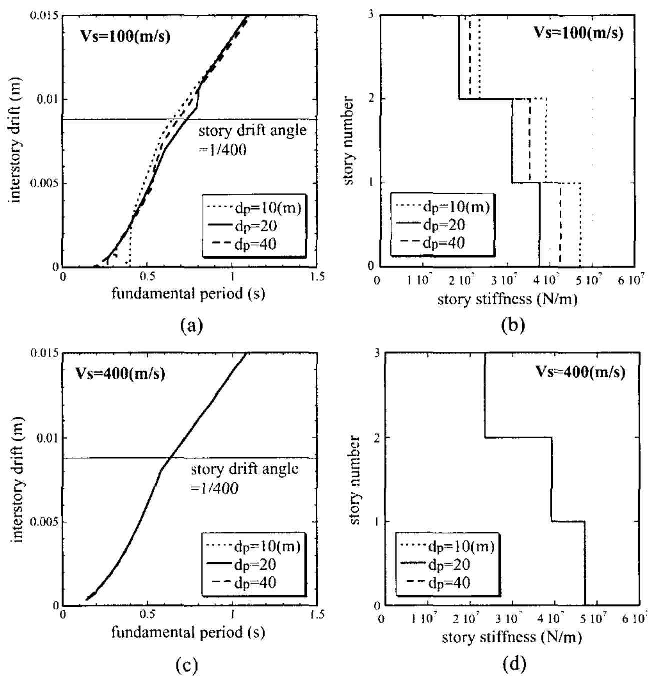

Fig. 8. 3-story model for various depths of soil layer: (a) interstory drift vs. fundamental period of interaction model (V_s=100(m/s)), (b) story stiffness (V_s=100(m/s)), (c) interstory drift vs. fundamental period of interaction model (V_s=400(m/s)), (d) story stiffness (V_s=400(m/s)).

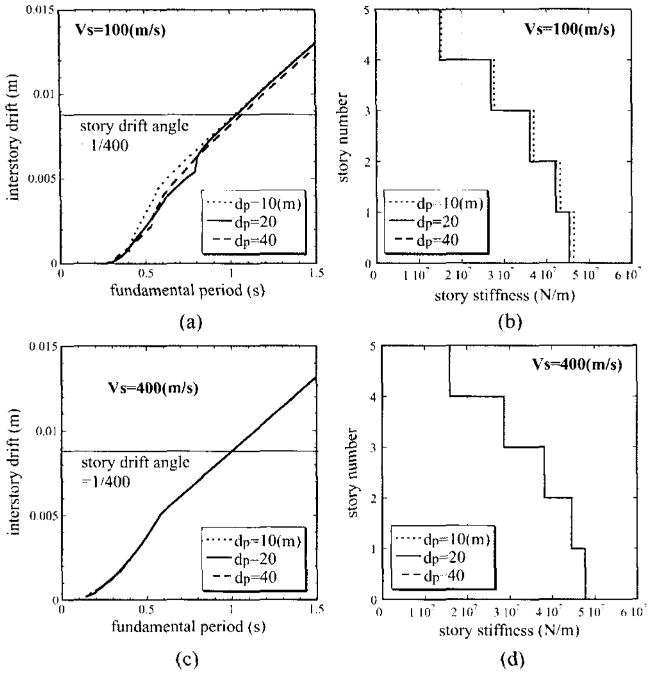

Fig. 9. 5-story model for various depths of soil layer: (a) interstory drift vs. fundamental period of interaction model (V_s= 100(m/s)), (b) story stiffness (V_s=100(m/s)), (c) interstory drift vs. fundamental period of interaction model (V_s=400(m/s)), (d) story stiffness (V_s=400(m/s)).

level of interstory drift is modified in a relatively small shear wave velocity (100 m/s), the order of the required story stiffnesses for various depths of soil layer changes irregularly.

Table 1 shows the lowest-mode damping ratio for the half-space model and the soil layer model. It can be observed that, when the soil shear wave velocity becomes large, the lowest-mode damping ratio approaches to the damping ratio 0.02 of the super-structure. However, there is no clear tendency on dependence of the damping ratio on the depth of soil layer in the soil layer model.

Table 1(a). Lowest-mode damping ratio for 3-story model

Half-space model		Soil layer model			
			d_p=10(m)	d_p=20(m)	d_p=40(m)
V_s=50(m/s)	0.092	V_s=50(m/s)	0.056	0.054	0.062
V_s=100	0.037	V_s=100	0.021	0.037	0.026
V_s=200	0.020	V_s=200	0.020	0.020	0.021
V_s=400	0.020	V_s=400	0.020	0.020	0.020

Table 1(b). Lowest-mode damping ratio for 5-story model

Half-space model		Soil layer model			
			d_p=10(m)	d_p=20(m)	d_p=40(m)
V_s=50(m/s)	0.056	V_s=50(m/s)	0.023	0.050	0.037
V_s=100	0.028	V_s=100	0.020	0.037	0.023
V_s=200	0.021	V_s=200	0.020	0.020	0.021
V_s=400	0.020	V_s=400	0.020	0.020	0.020

The accuracy of the present sway-rocking shear building model has been investigated extensively by the present authors (Nakamura and Takewaki, 1989b; Takewaki *et al.*, 2002). It has been shown that the present model is reasonably accurate in wide parameter ranges. This supports the reliability of the present design method together with the reasonable accuracy of the cone models.

6. Conclusions

The following conclusions may be drawn:

1. The design model of a building structure supported by a spring-dashpot system with impedance functions evaluated by the cone model can be a simple yet reasonably accurate model which can take into account the soil-structure interaction effects in usual structural design practice in a smart manner.
2. The formulation of inverse vibration problems for the design model with given impedance functions provides a useful design tool for finding story stiffnesses satisfying a stiffness performance condition. This formulation does not require eigenvalue analysis and enables one to trace efficiently various designs satisfying different performance conditions.
3. The following properties have been clarified by means of this formulation. (1) As the soil becomes stiffer, the influence of the ground properties on the design of super-structures becomes smaller; (2) As the soil becomes softer, story stiffnesses required for the given stiffness performance condition become smaller both in the half-space model and the soil layer model; (3) The half-space model requires smaller story stiffnesses than the soil layer model (small radiation damping in the frequency range below the cut-off frequency and strong frequency dependence of impedance functions are key factors); (4) The influence of the depth of soil layer on the super-structure design is not clear (the resonance between the soil layer vibration and the super-structure vibration may be a key issue).

It should be noted that the same design response spectrum defined at the ground surface level has been used regardless of the soil conditions in this paper. This treatment has been introduced to investigate purely the influence of the soil conditions (impedance functions) on the super-structure design. The simultaneous consideration of the influence of the soil conditions on the input design response spectrum and of the present analysis will lead to a more complete analysis of the SSI effects in the design problem.

Acknowledgements

The present work is partially supported by Grant-in-Aid for Scientific Research (No.12450225) from the Ministry of Education, Science, Sports and Culture of Japan and by the Secom Foundation (Tokyo).

References

Cakmak AS (ed.) (1987) Soil-structure interaction, Developments in Geotechnical Engineering 43, Elsevier and Computational Mechanics Publications.

Cakmak AS, Herrera I (eds.) (1989) Structural dynamics and soil structure interaction, Computational Mechanics Publications.

Cakmak AS, Abdel-Ghaffar AM, Brebbia CA (eds.) (1982) Soil dynamics and earthquake engineering, Vol. I, II, Proc. of the Conf. on Soil Dynamics and Earthquake Engineering, A.A. Balkema.

Der Kiureghian A (1980) Structural response to stationary excitation, J. Engng Mech, ASCE,106(EM6): 1195-1213.

Gupta VK, Trifunac MD (1991) Seismic response of multistoried buildings including the effects of soil-structure interaction, Soil Dynamics Earthquake Engng, 10(8): 414-422.

Kausel E, Manolis GD (eds.) (2000) Wave motion in earthquake engineering, WIT press.

Luco JE (1980) Linear soil-structure interaction, UCRL-15272, Lawrence Livermore Laboratory, Livermore, California.

Meek JW, Wolf JP (1994) Cone models for embedded foundation, J. Geotechnical Engng, ASCE, 120(1): 60-80.

Nakamura T, Takewaki I (1985) Optimum design of elastically supported shear buildings for constrained fundamental natural period, J. Struct. Engng., AIJ, 31B: 93-102 (in Japanese).

Nakamura T, Takewaki I (1989a) Optimal elastic structures with frequency-dependent elastic supports, Int. J. Solids Struct 25(5): 539-551.

Nakamura T, Takewaki I (1989b) Earthquake-response constrained design of pile-supported elastic shear buildings for site-dependent response spectra, Proc 9th World Conference on Earthquake Engng, V: 1043-1048.

Nakamura T, Takewaki I, Shimano Y (1992) Stiffness solution to a hybrid inverse seismic strain problem of a building frame-pile-soil system, J. Struct. Construction Engng, AIJ, 440: 43-56 (in Japanese).

Nakamura T, Takewaki I, Asaoka Y (1996) Sequential stiffness design for seismic drift ranges of a shear building-pile-soil system, Earthquake Engng Struct Dynamics, 25(12): 1405-1420.

Newmark NM, Hall WJ (1982) Earthquake spectra and design, Earthquake Engineering Research Institute.

Takewaki I (1998) Equivalent linear ductility design of soil-structure interaction systems, Engng Struct, 20(8): 655-662.

Takewaki I, Nakamura T (1995) Hybrid Inverse Mode Problems for FEM-Shear Models, J. Engng Mech, ASCE, 121(8): 873-880.

Takewaki I, Nakamura T (1997) Hybrid inverse mode problem for structure-foundation systems, J. Engng Mech ASCE, 123(4): 312-321

Takewaki I, Fujii N, Uetani K (2002) Simplified inverse stiffness design for nonlinear soil amplification, Engng Struct, 24(11): 1369-1381.

Takewaki I, Nakamura T, Hirayama K (1998) Seismic frame design via inverse mode design of frame-ground systems, Soil Dynamics Earthquake Engineering, 17(3): 153-163.

Wolf JP (1985) Dynamic soil-structure interaction, Prentice-Hall, Englewood Cliffs, NJ.

Wolf JP (1988) Soil-structure interaction analysis in time domain, Prentice-Hall, Englewood Cliffs, NJ.

Wolf JP (1994) Foundation vibration analysis using simple physical models, Prentice-Hall, Englewood Cliffs, NJ.

Appendix 1: Impedance functions via cone models (Meek and Wolf, 1994; Wolf, 1994)

[Half-space Model]
(Horizontal)

Let G, ν, ρ, V_S denote the soil shear modulus, Poisson's ratio, mass density and shear wave velocity. A_0 and r_0 are the foundation area and radius and Z_0 is defined in Fig. 1. The static horizontal stiffness of the cone model can be expressed by

$$K = \frac{GA_0}{z_0} = \frac{\rho V_S^2 A_0}{z_0} \tag{A1}$$

The static horizontal stiffness of the continuum model is obtained by

$$K = \frac{8Gr_0}{2-\nu} \tag{A2}$$

Equating (A1) and (A2) leads to the determination of the aspect ratio.

$$\frac{z_0}{r_0} = \frac{\pi}{8}(2-\nu) \tag{A3}$$

The horizontal spring coefficient and dashpot damping coefficient can then be expressed by

$$k_H = K \tag{A4a}$$

$$c_H = K\frac{z_0}{V_S} \tag{A4b}$$

(Rocking)

Let I_0 denote the second moment of foundation area. The static rotational (rocking) stiffness of the cone model can be expressed by

$$K_\theta = \frac{3\rho V^2 I_0}{z_0} \tag{A5}$$

The static rotational (rocking) stiffness of the continuum model is obtained by

$$K_\theta = \frac{8Gr_0^3}{3(1-\nu)} \tag{A6}$$

Equating (A1) and (A2) leads to the determination of the aspect ratio.

$$\frac{z_0}{r_0} = \frac{9\pi}{32}(1-\nu)\left(\frac{V}{V_S}\right)^2 \tag{A7}$$

Let us define the following function.

$$S_\theta(\omega) = \left\{1 - \frac{4}{3}\frac{\mu_\theta z_0}{\pi r_0}\left(\frac{V_S}{V}\right)^2 a_0^2 - \frac{1}{3}\frac{a_0^2}{\left(\frac{r_0 V}{z_0 V_S}\right)^2 + a_0^2}\right\} + ia_0\left\{\frac{z_0 V_S}{3r_0 V}\frac{a_0^2}{\left(\frac{r_0 V}{z_0 V_S}\right) + a_0}\right\} \tag{A8}$$

where $a_0 = \omega r_0 / V_S$ and

$$\mu_\theta = 0,\quad V = V_P\ (\nu \le 1/3) \tag{A9a}$$

$$\mu_\theta = 0.3\pi(\nu - (1/3)),\quad V = 2V_S\ (1/3 < \nu \le 1/2) \tag{A9b}$$

V_P is the longitudinal wave propagation velocity. The rotational (rocking) spring coefficient and dashpot damping coefficient can then be expressed by

$$k_R = K_\theta Re(S_\theta) \tag{A10a}$$

$$c_R = K_\theta \frac{Im(S_\theta)}{\omega} \tag{A10b}$$

[Soil Layer Model]

(Horizontal)

Let d_P denote the depth of soil layer. Let us define the following function.

$$S(\omega) = \frac{1 + i\frac{\omega T}{\kappa}}{\sum_{j=0}^{\infty} e_j^F e^{ij\omega T}} \tag{A11}$$

where

$$T = \frac{2d_P}{V_S},\quad \kappa = \frac{2d_P}{z_0} \tag{A12a, b}$$

$$e_0^F = 1,\quad e_j^F = \frac{2(-1)^j}{1 + j\kappa}\ (j \ge 1) \tag{A13a, b}$$

The horizontal spring coefficient and dashpot damping coefficient can then be expressed by

$$k_H = KRe(S) \tag{A14a}$$

$$c_H = K\frac{Im(S)}{\omega} \tag{A14b}$$

where K is the static horizontal stiffness for the soil layer model.

(Rocking)

Let us define the following function.

$$S_\theta(\omega) = \frac{1 - \frac{1}{3}\frac{(\omega T)^2}{\kappa^2 + (\omega T)^2} + i\frac{\omega T}{3\kappa}\frac{(\omega T)^2}{\kappa^2 + (\omega T)^2}}{1 + \frac{2}{1 + i\frac{\omega T}{\kappa}}\left\{\sum_{j=1}^{\infty}(-1)^j \frac{e^{-ij\omega T}}{(1 + j\kappa)^3} + i\frac{\omega T}{\kappa}\sum_{j=1}^{\infty}(-1)^j \frac{e^{-ij\omega T}}{(1 + j\kappa)^2}\right\}} \tag{A15}$$

$$T = \frac{2d_P}{V},\quad k = \frac{2d_P}{z_0} \tag{A16a, b}$$

$$V = V_P\ (\nu \le 1/3),\quad V = 2V_S\ (1/3 < \nu \le 1/2) \tag{A17a, b}$$

The rotational (rocking) spring coefficient and dashpot damping coefficient can then be expressed by

$$k_R = K_\theta Re(S_\theta) \tag{A18a}$$

$$c_R = K_\theta \frac{Im(S_\theta)}{\omega} \tag{A18b}$$

where K_θ is the static rotational stiffness for the soil layer model.

Appendix 2: Story Stiffnesses of the Shear Building with a Specified Lowest Eigenvalue and a Uniform Distribution of Lowest-Mode Interstory Drifts (Nakamura and Takewaki, 1985)

Let $\bar{\Omega}_1$ denote the specified lowest eigenvalue of the interaction model which can be expressed as $\bar{\Omega}_1 = (2\pi/T_1)^2$ in terms of the fundamental period T_1. The story stiffnesses of the model can be obtained from

$$k_j = \overline{\Omega}_1 \sum_{i=j}^{f} m_i(U_F + \Theta_F H_i + i) \quad (j = 1, 2, \ldots, f) \qquad \text{(A19)}$$

H_i is defined in equation (4d). U_F and Θ_F are given by

$$U_F = \frac{D_2 D_5 - D_3 D_4}{D_1 D_4 - D_2^2}, \quad \Theta_F = \frac{D_2 D_3 - D_1 D_5}{D_1 D_4 - D_2^2} \qquad \text{(A20a, b)}$$

where

$$D_1 = E_1 - \frac{\bar{k}_H}{\overline{\Omega}_1}, \quad D_2 = E_2, \quad D_3 = \sum_{i=1}^{f} i m_i$$

$$D_4 = E_3 - \frac{\bar{k}_R}{\overline{\Omega}_1}, \quad D_5 = \sum_{i=1}^{f} i m_i H_i \qquad \text{(A21a-e)}$$

The symbols E_1, E_2, E_3 are defined in equations (4a-c).